

Coded Computation Against Straggling Decoders for Network Function Virtualization

Malihe Aliasgari*, Jörg Kliewer*, and Osvaldo Simeone†

* Helen and John C. Hartmann Department of Electrical and Computer Engineering
New Jersey Institute of Technology, Newark, New Jersey 07102-1982
{ma839, jkliewer}@njit.edu

† Department of Informatics, King's College London, London, UK
osvaldo.simeone@kcl.ac.uk

Abstract—The uplink of a cloud radio access network (C-RAN) architecture is studied in which decoding at the cloud takes place via Network Function Virtualization (NFV) on commercial off-the-shelf (COTS) servers. In order to mitigate the impact of straggling decoders in the cloud computing platform, a novel coding strategy is proposed, whereby the cloud re-encodes the received frames via a linear code before distributing them to the decoding processors. Upper bounds on the resulting Frame Error Rate (FER) as a function of the decoding latency are derived by assuming a binary symmetric channel for uplink communications. The bounds leverage large deviation results for correlated variables, and depend on the properties of both the uplink linear channel code adopted at the user and the NFV linear code applied at the cloud. Numerical examples demonstrate that the bounds are useful tools for code design, and that coding is instrumental in obtaining a desirable trade-off between FER and decoding latency.

Index Terms—Coded computation, network function virtualization, C-RAN, large deviation.

I. INTRODUCTION

Promoted by the European Telecommunications Standards Institute (ETSI), Network Function Virtualization (NFV) has become a cornerstone of the envisaged architecture of 5G systems [1]. NFV leverages virtualization technologies in order to implement network functionalities on commercial off-the-shelf (COTS) programmable hardware, such as general purpose servers, potentially reducing both capital and operating costs. An important challenge in the deployment of NFV is ensuring carrier grade performance while relying on COTS components. Such components may be subject to temporary unavailability due to malfunctioning, and are generally characterized by randomness in their execution runtimes [2]. The typical solution to these problems involves replicating the Virtual Machines (VMs) that execute given network functions on multiple processors, e.g., cores or servers [2]–[5].

The problem of straggling processors, that is, of processors lagging behind in the execution of a certain orchestrated function, has been well studied in the context of distributed computing [6]. Recently, it has been pointed out that, for the important case of linear functions, it is possible to improve

over repetition strategies in terms of the trade-off between performance and latency by carrying out linear precoding of the data prior to processing [7]–[12]. The key idea is that, by employing suitable linear (erasure) block codes operating over fractions of size $1/K$ of the original data, a function may be completed as soon as a number of K or more processors, depending on the minimum distance of the code, has finalized its operation, irrespective of their identity.

In this paper we consider the function of decoding in the uplink of a Cloud Radio Access Network (C-RAN). As shown in Fig. 1, in a C-RAN system decoding takes place at the cloud. Keeping the decoding latency to a minimum is a major challenge in the implementation of C-RAN owing to timing constraints from the MAC layer retransmission protocol [13]. Reference [13] argued that exploiting parallelism across multiple cores in the cloud can reduce the overall decoding latency. However, parallel processing alone does not address the discussed unreliability of COTS hardware. In [14], it was hence proposed to perform linear precoding of the received frames at the cloud in order to mitigate the impact of unreliable decoding servers.

In this paper we extend the treatment of linear coding against unreliable processors in the C-RAN uplink in the following ways. First, while reference [14] considered only a toy example with three processors, here we generalize the approach to any number of processors. Second, unlike the simple binary availability model of [14], in which a processor is either on or off, here we adopt a set-up in which the computing runtime of each processor is random and generally dependent on the computational load as in, e.g., [7], [8]. Third, while [14] relied solely on numerical results, here we develop two analytical upper bounds on the FER as a function of the decoding delay. The bounds leverage large deviation results for correlated variables [15], and depend on the properties of both the uplink linear channel code adopted at the user and the NFV linear code applied at the cloud. Further, as a byproduct of the analysis, we introduce the dependency graph of a linear code and its chromatic number as novel relevant parameters of a linear code beside the minimum distance, blocklength, and rate.

The rest of the paper is organized as follows. In Sec. II, we present the system model focusing, as in [14], on a Binary

This work was supported in part by U.S. NSF grants CNS-1526547 and CCF-1525629. O. Simeone has also received funding from the European Research Council (ERC) under the European Unions Horizon 2020 research and innovation programme (grant agreement No 725731).

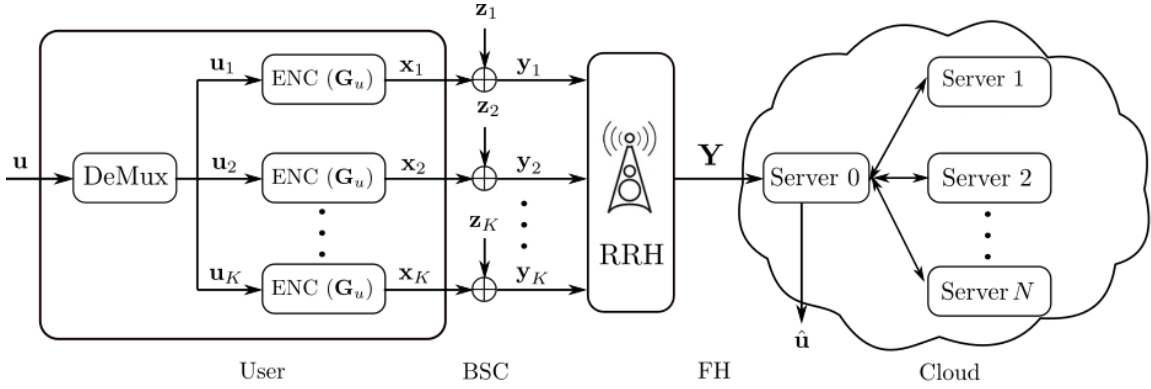


Fig. 1: NfV model for uplink channel decoding. The input file \mathbf{u} is divided into smaller packets and encoded with a linear code \mathcal{C}_u having generator matrix \mathbf{G}_u . The packets are received by the RRH through a BSC and forwarded to a cloud. Server 0 in the cloud re-encodes the received packet with a linear code \mathcal{C}_c in order to enhance robustness against the potentially straggling servers $1, \dots, N$.

Symmetric Channel (BSC) for uplink communications. Sec. III presents the two proposed upper bounds on the Frame Error Rate (FER), and Sec. IV provides numerical results.

II. SYSTEM MODEL

As illustrated in Fig. 1, we consider the uplink of a C-RAN system in which a user communicates with the cloud via a remote radio head (RRH). The user is connected to the RRH via a BSC with bit flipping probability δ , while the RRH-to-cloud link, typically referred to as fronthaul, is assumed to be noiseless. Note that the BSC is a simple model for the uplink channel, while the noiseless fronthaul accounts for a typical deployment with higher capacity fiber optic cables. The cloud contains a master server, or server 0, and N slave servers, i.e., servers $1, \dots, N$. The slave servers are characterized by random computing delays as in related works on coded computation [7], [8], [12]. Note that we use here the term “server” to refer to a decoding processor, although, in a practical implementation, this may correspond to a core of the cloud computing platform [13].

The user encodes a file \mathbf{u} consisting L bits. Before encoding, the file is divided into K blocks $\mathbf{u}_1, \mathbf{u}_2, \dots, \mathbf{u}_K \in \{0, 1\}^{L/K}$ of equal size, each of them containing L/K bits. As shown in Fig. 1, in order to combat noise on the BSC, the transmitted frames are encoded by an (n, k) binary linear code \mathcal{C}_u of rate $r = k/n$ defined by generator matrix $\mathbf{G}_u \in \mathbb{F}_2^{n \times k}$, where $n = L/(rK)$ and $k = L/K$. Let $\mathbf{x}_j \in \{0, 1\}^n$ with $j \in \{1, \dots, K\}$ be the K transmitted packets of length n . At the output of the BSC, the length- n received vector for the j th packet at the RRH is given as

$$\mathbf{y}_j = \mathbf{x}_j \oplus \mathbf{z}_j, \quad (1)$$

where \mathbf{z}_j is a vector of i.i.d. Bern(δ) random variables (rvs). The K received packets $(\mathbf{y}_1, \mathbf{y}_2, \dots, \mathbf{y}_K)$ by the RRH are transmitted to the cloud via the fronthaul link, and the cloud performs decoding. Specifically, as detailed next, we assume that each server $1, \dots, N$ performs decoding of a single packet of length n bits while server 0 acts as coordinator.

Assuming the overprovisioning of servers, which entails the condition $N \geq K$, we adopt the idea of NfV coding proposed in [14]. Accordingly, as seen in Fig. 2, the K packets are first linearly encoded by server 0 into $N \geq K$ coded blocks

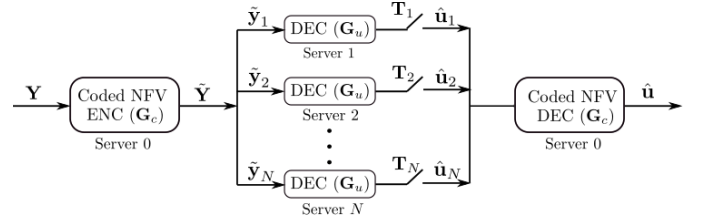


Fig. 2: Coded NfV at the cloud: Server 0 re-encodes the received packets in \mathbf{Y} by a linear NfV code \mathcal{C}_c with generator \mathbf{G}_c . Each encoded packet $\tilde{\mathbf{y}}_i$ then conveyed to server i for decoding.

of the same length n bits, each forwarded to a different server for decoding. This form of encoding is meant to mitigate the effect of straggling servers in a manner similar to [7], [8], [12]. Using an (N, K) linear code \mathcal{C}_c with $K \times N$ generator matrix $\mathbf{G}_c \in \mathbb{F}_2^{N \times K}$, the encoded packets are obtained as

$$\tilde{\mathbf{Y}} = \mathbf{Y} \mathbf{G}_c, \quad (2)$$

where $\mathbf{Y} = [\mathbf{y}_1, \dots, \mathbf{y}_K]$ is the $n \times K$ matrix obtained by including the received signal \mathbf{y}_j as the j th column and $\tilde{\mathbf{Y}} = [\tilde{\mathbf{y}}_1, \dots, \tilde{\mathbf{y}}_N]$ is the $n \times N$ matrix whose i th column $\tilde{\mathbf{y}}_i$ is the input to server i , where $i \in \{1, \dots, N\}$. From (1), this vector can be written as

$$\tilde{\mathbf{y}}_i = \sum_{j=1}^K \mathbf{y}_j g_{c,ji} = \sum_{j=1}^K \mathbf{x}_j g_{c,ji} + \sum_{j=1}^K \mathbf{z}_j g_{c,ji}, \quad (3)$$

where $g_{c,ji}$ is the (j, i) entry of matrix \mathbf{G}_c .

The signal part $\sum_{j=1}^K \mathbf{x}_j g_{c,ji}$ in (3) is a linear combination of d_i codewords for the rate- r binary code with generator matrix \mathbf{G}_u , and hence it is a codeword of the same code. The parameter d_i , $i \in \{1, \dots, N\}$, denotes the Hamming weight of the i th column of matrix \mathbf{G}_c , where $0 \leq d_i \leq K$. Each server i receives as input the packets $\tilde{\mathbf{y}}_i$ from which it can decode the codeword $\sum_{j=1}^K \mathbf{x}_j g_{c,ji}$. This decoding operation is affected by the noise vector $\sum_{j=1}^K \mathbf{z}_j g_{c,ji}$ in (3), which has i.i.d. Bern(γ_i) elements. Here γ_i is obtained as the first row and second column's entry of the matrix \mathbf{Q}^{d_i} , with \mathbf{Q} being the channel matrix $\mathbf{Q} = (1 - 2\delta) \mathbf{I} + \delta \mathbf{1} \mathbf{1}^T$ (\mathbf{I} is the identity matrix and $\mathbf{1}$ the all-one column vector). Note that a larger value of d_i yields a larger bit flipping probability γ_i . We define

as $P_{n,k}(\gamma_i)$ the decoding error probability of server i , which can be upper bounded by [16, Theorem 33].

Server i requires a random time $T_i = T_{1,i} + T_{2,i}$ to complete decoding, which is modeled as the sum of a component $T_{1,i}$ that is independent of the workload and a component $T_{2,i}$ that instead grows with the size n of the packet processed at each server, respectively. The first component accounts, e.g., for processor unavailability periods, while the second models the execution runtime from the start of the computation. The first variable $T_{1,i}$ is assumed to have an exponential probability density function (pdf) $f_1(t)$ with mean $1/\mu_1$, while the variable $T_{2,i}$ has a shifted exponential distribution with cumulative distribution function (cdf) [17]

$$F_2(t) = 1 - \exp\left(-\frac{rK\mu_2}{L}\left(t - a\frac{L}{rK}\right)\right), \quad (4)$$

for $t \geq aL/(rK)$ and $F_2(t) = 0$ otherwise. The parameter a represents the minimum processing time per input bit, while $1/\mu_2$ is the average additional time needed to process one bit. The cdf of the time T_i can hence be written as the integral $F(t) = \int_0^t f_1(\tau)F_2(t-\tau)d\tau$. We also assume that the runtime rvs $\{T_i\}_{i=1}^N$ are mutually independent. Due to (4), the probability that a given set of l out of N servers has finished decoding by time t is given as

$$a_l(t) = F(t)^l(1 - F(t))^{N-l}. \quad (5)$$

Let d_{\min} be the minimum distance of the NRV code \mathcal{C}_c . Due to (3), server 0 in the cloud is able to decode the message \mathbf{u} or equivalently the K packets \mathbf{u}_j for $j \in \{1, \dots, K\}$, as soon as $N - d_{\min} + 1$ servers have decoded successfully. Let $\hat{\mathbf{u}}_i$ be the output of the i th server in the cloud upon decoding. The output $\hat{\mathbf{u}}$ of the decoder at server 0 at time t is then a function of the vectors $\hat{\mathbf{u}}_i(t)$ for $i \in \{1, \dots, N\}$, where

$$\hat{\mathbf{u}}_i(t) = \begin{cases} \hat{\mathbf{u}}_i, & \text{if } T_i \leq t, \\ \emptyset, & \text{otherwise.} \end{cases}$$

Finally, the frame error rate (FER) at time t is defined as the probability

$$P_e(t) = \Pr[\hat{\mathbf{u}}(t) \neq \mathbf{u}]. \quad (6)$$

III. LARGE DEVIATION BOUND ON THE FRAME ERROR PROBABILITY

In this section we derive analytical bounds on the error probability $P_e(t)$ in (6).

A. Preliminaries

Each server i with $i \in \{1, \dots, N\}$ decodes successfully its assigned packet $\tilde{\mathbf{y}}_i$ if: (i) the server completes decoding by time t ; (ii) the decoder is able to correct the errors caused by the BSC. Furthermore as discussed, an error occurs at time t if the number of servers that have successfully decoded by time t is smaller than $N - d_{\min} + 1$. To evaluate the FER, we hence define the indicator variables $C_i(t) = \mathbb{1}\{T_i \leq t\}$ and $D_i = \mathbb{1}\{\hat{\mathbf{u}}_i = \mathbf{u}_i\}$, which are equal to 1 if the events (i) and

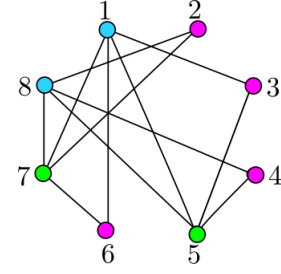


Fig. 3: Dependency graph associated with an (8,4) NRV code \mathcal{C}_c in Example 1.

(ii) described above occur, respectively, and zero otherwise. Based on these definitions, the FER is equal to

$$P_e(t) = \Pr\left[\sum_{i=1}^N C_i(t)D_i \leq N - d_{\min}\right]. \quad (7)$$

The indicator variables $C_i(t)$ are independent Bernoulli rvs across the servers $i \in \{1, \dots, N\}$, due to the independence assumption on the rvs T_i . However, the indicator variable D_i are dependent Bernoulli rvs. The dependence of the variables D_i is caused by the fact that the noise terms $\sum_{i=1}^K \mathbf{z}_j g_{c,ji}$ in (3) generally have common terms. In particular, if two columns i and j of the generator matrix \mathbf{G}_c have at least a 1 in the same row, then the decoding indicators D_i and D_j are correlated. This complicates the evaluation of bounds on the FER (7).

B. Dependency Graph and Chromatic Number of a Linear Code

To capture the correlation among the indicator variables D_i , we introduce here the notion of the *dependency graph* and its chromatic number for a linear code. These appear to be novel properties of a linear code, which will be argued below to determine a code's performance for the application at hand.

Definition 1. Let $\mathbf{G} \in \mathbb{F}_2^{K' \times N'}$ be a generator matrix of a linear code. The dependency graph $\mathcal{G}(\mathbf{G}) = (\mathcal{V}, \mathcal{E})$ comprises a set \mathcal{V} of N' vertices and a set $\mathcal{E} \subseteq \mathcal{V} \times \mathcal{V}$ of edges, where edge $(i, j) \in \mathcal{E}$ is included if both the i th and j th columns of \mathbf{G} have at least a 1 in the same row.

Example 1. For an (8,4) NRV code \mathcal{C}_c with the following generator matrix

$$\mathbf{G}_c = \begin{bmatrix} 1 & 0 & 0 & 0 & 0 & 1 & 1 & 0 \\ 0 & 0 & 0 & 1 & 1 & 0 & 0 & 1 \\ 0 & 1 & 0 & 0 & 0 & 0 & 1 & 1 \\ 1 & 0 & 1 & 0 & 1 & 0 & 0 & 0 \end{bmatrix}, \quad (8)$$

Fig. 3 shows the resulting dependency graph $\mathcal{G}(\mathbf{G}_c)$.

The chromatic number $\chi(\mathbf{G})$ of the graph $\mathcal{G}(\mathbf{G})$ will play an important role in the analysis. We recall that the chromatic number is the smallest number of colors needed to color the vertices of $\mathcal{G}(\mathbf{G})$, such that no two adjacent vertices share the same color (see example in Fig. 3). Generally, finding the chromatic number of a graph is NP-hard [18]. However, a simple upper bound on $\chi(\mathbf{G})$ is given as [19]

$$\chi(\mathbf{G}) \leq \Delta(\mathbf{G}) + 1, \quad (9)$$

where $\Delta(\mathbf{G})$ is the maximum degree of a graph $\mathcal{G}(\mathbf{G})$.

C. Large Deviation Upper Bound

In this subsection, we provide a first upper bound on the FER. The bound is based on the large deviation result in [15] for the tail probabilities of rvs $X = \sum_{i=1}^M X_i$, where the rvs X_i are generally dependent. The correlation of rvs $\{X_i\}$ is described in [15] by a dependency graph. This is defined as any graph $\mathcal{G}(X)$ with X_i as vertices, such that, if a vertex $i \in \{1, \dots, M\}$ is not connected to any vertex in a subset $\mathcal{J} \subset \{1, \dots, M\}$, then X_i is independent of $\{X_j\}_{j \in \mathcal{J}}$.

Lemma 1 ([15]). *Let $X = \sum_{i=1}^M X_i$, where $X_i \sim \text{Bern}(p_i)$ and $p_i \in (0, 1)$ are generally dependent. For any $b \geq 0$, such that the inequality $X_i - \mathbb{E}(X_i) \geq -b$ holds for all $i \in \{1, \dots, M\}$ with probability one, and for any $\tau \geq 0$ we have*

$$\Pr[X \leq \mathbb{E}(X) - \tau] \leq \exp\left(-\frac{S}{b^2 \mathcal{X}(\mathcal{G}(X))} \varphi\left(\frac{4b\tau}{5S}\right)\right), \quad (12)$$

where $S \triangleq \sum_{i=1}^N \text{Var}(X_i)$ and $\varphi(x) \triangleq (1+x) \ln(1+x) - x$. The same bound (12) holds for $\Pr[X \geq \mathbb{E}(X) + \tau]$, where $X_i - \mathbb{E}(X_i) \leq b$ with probability one.

The following theorem uses Lemma 1 to derive a bound on the FER.

Theorem 1. *Let $P_{n,k}^{\min} = \min_i \{P_{n,k}(\gamma_i)\}_{i=1}^N$. Then, for all*

$$t \geq n \left(a - \frac{1}{\mu} \ln \left(\frac{d_{\min} - \sum_{i=1}^N P_{n,k}(\gamma_i)}{N - \sum_{i=1}^N P_{n,k}(\gamma_i)} \right) \right), \quad (13)$$

the FER is upper bounded as in (10), shown at the bottom of the page, where $b(t) \triangleq F(t) (1 - P_{n,k}^{\min}) - 1$ and $S(t) \triangleq \sum_{i=1}^N F(t) (1 - P_{n,k}(\gamma_i)) (1 - F(t)(1 - P_{n,k}(\gamma_i)))$.

Proof. Let $X_i(t) \triangleq C_i(t)D_i$ and $X(t) = \sum_{i=1}^N X_i(t)$, where $X_i(t)$ are dependent Bernoulli rvs with probability $\mathbb{E}[X_i(t)] = \Pr[X_i(t) = 1] = F(t) (1 - P_{n,k}(\gamma_i))$. It can be seen that a valid dependency graph $\mathcal{G}(X)$ for the variables $\{X_i\}$ is the dependency graph $\mathcal{G}(\mathbf{G}_c)$ defined above. This is due to the fact, discussed in Section III-C, that the rvs X_i and X_j are dependent if and only if the i th and j th column of \mathbf{G}_c have at least a 1 in a common row. We can hence apply Lemma 1 for every time t by selecting $\tau = \mathbb{E}(X) - N + d_{\min}$, and $b(t)$ as defined above. Note that this choice of $b(t)$ meets the constraint for b in Lemma 1. \square

The upper bound (10), on the FER captures the dependency of the FER on both the channel code and the NFV code.

In particular, the bound is an increasing function of the error probabilities $P_{n,k}(\gamma_i)$, which depend on both codes. It also depends on the NFV code through parameters d_{\min} and $\mathcal{X}(\mathbf{G}_c)$.

D. Union Bound

As indicated in Theorem 1, the large deviation based bound in (10) is only valid for large enough t , as can be observed from (13). Furthermore, it may generally not be tight, since it neglects the independence of the indicator variables D_i . In this subsection, a generally tighter but more complex bound is derived that is valid for all times t .

Theorem 2. *For any subset $\mathcal{A} \subseteq \{1, \dots, N\}$, define*

$$P_{n,k}^{\min(\mathcal{A})} \triangleq \min\{P_{n,k}(\gamma_i)\}_{i \in \mathcal{A}} \quad \text{and} \quad P_{n,k}^{\mathcal{A}} \triangleq \sum_{i \in \mathcal{A}} P_{n,k}(\gamma_i),$$

and let $\mathbf{G}_{\mathcal{A}}$ be the $K \times |\mathcal{A}|$ submatrix of \mathbf{G}_c , with column indices in the subset \mathcal{A} . Then, the FER is upper bounded by (11), shown at the bottom of the page, where $S_{\mathcal{A}}(t) \triangleq \sum_{i \in \mathcal{A}} P_{n,k}(\gamma_i) (1 - P_{n,k}(\gamma_i))$ and $b_{\mathcal{A}} \triangleq 1 - P_{n,k}^{\min(\mathcal{A})}$.

Proof. Let $I_i = 1 - D_i$ be the indicator variable which equals 1 if server i fails decoding. Accordingly, we have $I_i \sim \text{Bern}(P_{n,k}(\gamma_i))$. For each subset $\mathcal{A} \subseteq \{1, \dots, N\}$, let $I_{\mathcal{A}} = \sum_{i \in \mathcal{A}} I_i$. The complement of the FER $P_s(t) = 1 - P_e(t)$ can hence be written as

$$P_s(t) = \Pr \left[\sum_{i=1}^N C_i(t) D_i > N - d_{\min} \right] \quad (14)$$

$$= \sum_{l=N-d_{\min}+1}^N a_l(t) \sum_{\substack{\mathcal{A} \subseteq \{1, \dots, N\}: \\ |\mathcal{A}|=l}} (1 - \Pr[I_{\mathcal{A}} \geq l - N + d_{\min}]). \quad (15)$$

We can now apply Lemma 1 to the probability in (15) by noting that $\mathcal{G}(\mathbf{G}_{\mathcal{A}})$ is a valid dependency graph for the variables $\{I_i\}$, $i \in \mathcal{A}$. In particular, we apply Lemma 1 by setting $\tau_{\mathcal{A}} = l - N + d_{\min} - \mathbb{E}(I_{\mathcal{A}})$, $b_{\mathcal{A}} \geq I_i - \mathbb{E}[I_i]$, and $S_{\mathcal{A}} = \sum_{i \in \mathcal{A}} \text{Var}(I_i)$, leading to

$$\Pr[I_{\mathcal{A}} \geq l - N + d_{\min}] \leq \exp \left(-\frac{S_{\mathcal{A}}}{b_{\mathcal{A}}^2 \mathcal{X}(\mathbf{G}_{\mathcal{A}})} \varphi \left(\frac{4b_{\mathcal{A}} (l - N + d_{\min} - P_{n,k}^{\mathcal{A}})}{5S_{\mathcal{A}}} \right) \right). \quad (16)$$

By substituting (16) into (15), the proof is completed. \square

$$P_e(t) \leq \exp \left(-\frac{S(t)}{b^2(t) \mathcal{X}(\mathbf{G}_c)} \varphi \left(\frac{4b(t) (NF(t) - F(t) \sum_{i=1}^N P_{n,k}(\gamma_i) - N + d_{\min})}{5S(t)} \right) \right), \quad (10)$$

$$P_e(t) \leq 1 - \sum_{l=N-d_{\min}+1}^N a_l(t) \sum_{\substack{\mathcal{A} \subseteq \{1, \dots, N\}: \\ |\mathcal{A}|=l}} \left(1 - \exp \left(-\frac{S_{\mathcal{A}}}{b_{\mathcal{A}}^2 \mathcal{X}(\mathbf{G}_{\mathcal{A}})} \varphi \left(\frac{4b_{\mathcal{A}} (l - N + d_{\min} - P_{n,k}^{\mathcal{A}})}{5S_{\mathcal{A}}} \right) \right) \right). \quad (11)$$

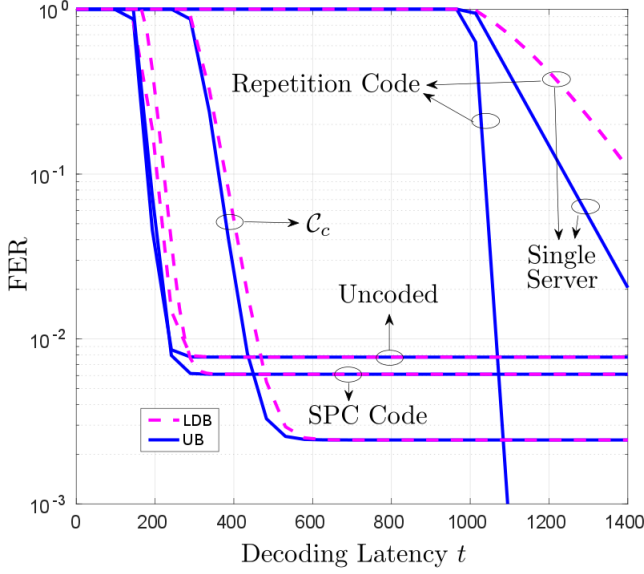


Fig. 4: Large deviation (LDB) bound of Theorem 1 and union bound (UB) in Theorem 2 for single-server decoding, repetition coding, uncoded approach, SPC code and the NfV code C_c defined in (8) ($L = 504, N = 8, 1/\mu_1 = 0, \mu_2 = 10, a = 1, \delta = 0.01, r = 0.5$).

IV. SIMULATION RESULTS

In this section we provide some numerical result to validate the two bounds presented in Theorems 1 and 2, as well as to assess the importance of coding in obtaining desirable trade-offs between decoding latency and FER. We employ a frame length of $L = 504$ and $N = 8$ servers. The user code C_u is selected to be a randomly designed $(3, 6)$ regular (Gallager-type) LDPC code with $r = 0.5$, which is decoded via belief propagation.

Figures 4, 5, 6, and 7 compare the performance of the following solutions: (i) *Standard single-server decoding*, whereby we assume the use of a single server, that is $N = 1$, that decodes the entire frame ($K = 1$); (ii) *Repetition coding*, whereby the entire frame ($K = 1$) is replicated at all servers; (iii) *Parallel (or uncoded) processing*, whereby the frame is divided into $K = N$ disjoint parts processed by different servers; (iv) *Single parity check code (SPC)*, with $K = 7$, whereby one server decodes a binary sum of all other K received packets; and (v) an NfV code C_c with the generator matrix \mathbf{G}_c defined in (8), which is instead characterized by $K = 4$.

Note that, with both single-server decoding and repetition coding, we have the blocklength $n = 1008$ for the channel code. Single-server decoding is trivially characterized by $\mathcal{X}(\mathbf{G}_c) = d_{\min} = 1$, while repetition coding is such that the equalities $\mathcal{X}(\mathbf{G}_c) = d_{\min} = 8$ hold. Furthermore, the uncoded approach is characterized by $n = 126, d_{\min} = 1$ and $\mathcal{X}(\mathbf{G}_c) = 1$; the SPC code has $n = 144, d_{\min} = 2$ and $\mathcal{X}(\mathbf{G}_c) = 2$; and the NfV code C_c has $n = 252, d_{\min} = 3$ and $\mathcal{X}(\mathbf{G}_c) = 3$. The exact FER for a given function $P_{n,k}(\cdot)$ can easily be computed for cases (i)-(iii). In particular, for single

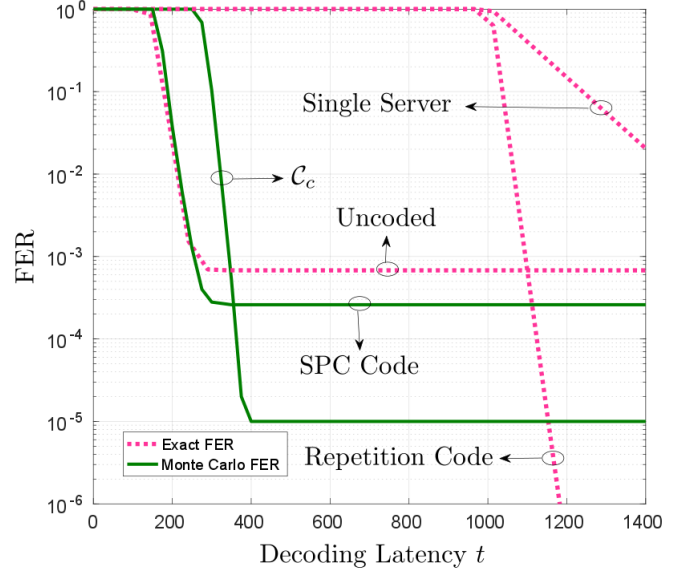


Fig. 5: Exact FER for single-server decoding, repetition coding, uncoded approach and Monte Carlo simulation results for the SPC code and the NfV code C_c defined in (8) ($L = 504, N = 8, 1/\mu_1 = 0, \mu_2 = 10, a = 1, \delta = 0.01, r = 0.5$).

server decoding, the FER equals

$$P_e(t) = 1 - a_1(t)(1 - P_{L/r,L}(\delta)); \quad (17)$$

for the repetition code, the FER is

$$P_e(t) = 1 - \sum_{i=1}^N a_i(t)(1 - P_{L/r,L}(\delta)); \quad (18)$$

and with the uncoded approach, we have

$$P_e(t) = 1 - a_N(t)(1 - P_{L/(rN),L/N}(\delta))^N. \quad (19)$$

Note that the exact FER for the NfV code SPC code and C_c is difficult to compute owing to the discussed correlation among the decoding outcomes at the servers.

In Fig. 4 and Fig. 5, we assume that the latency contribution that is independent of the workload is negligible, i.e., $1/\mu_1 = 0$. In Fig. 6 and Fig. 7, we consider instead a case with a positive value for $1/\mu_1$, in which latency may be dominated by effects that are independent of n .

Fig. 4 shows both LDB in Theorem 1 and UB in Theorem 2, respectively, for all five schemes, $1/\mu_1 = 0, a = 1$, and $\mu_2 = 10$. As a first observation, Fig. 4 confirms that the UB bound is tighter than the LDB. Furthermore, we note that leveraging multiple servers in parallel for decoding yields significant gains in terms of the trade-off between latency and FER as argued also in [13] using experimental results. With regard to the comparison among different NfV coding schemes, we first observe that the bounds indicate that the uncoded scheme is to be preferred for lower latencies. This is due to the shorter blocklength n , which entails a smaller average decoding time. However, the error floor of the uncoded scheme is large given the higher error probability on the

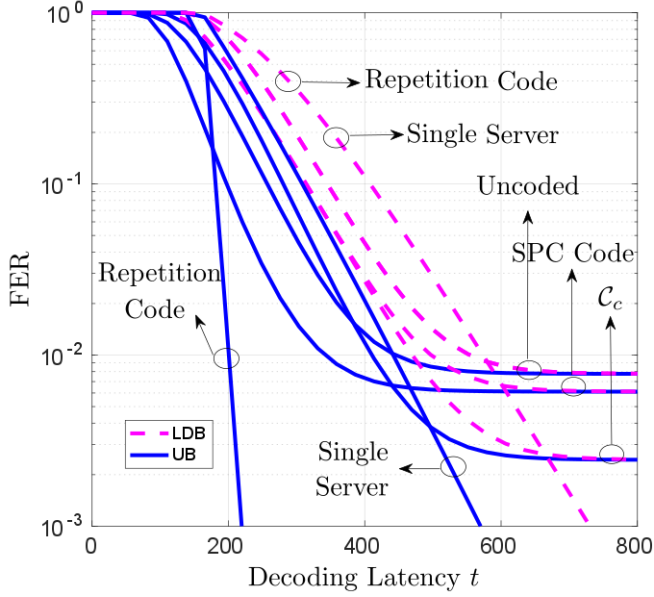


Fig. 6: Large deviation (LDB) bound of Theorem 1 and union bound (UB) in Theorem 2 for single-server decoding, repetition coding, uncoded approach, SPC code and the NfV code C_c defined in (8) ($L = 504, N = 8, 1/\mu_1 = 50, \mu_2 = 20, a = 0.1, \delta = 0.01, r = 0.5$).

BSC for short blocklengths. In contrast, repetition coding requires a larger latency in order to obtain acceptable FER performance owing to the larger blocklength n , but it achieves a significantly lower error floor. For intermediate latencies, SPC, and at larger latencies also the NfV code C_c , provide a lower FER according to the bounds. This suggests the effectiveness of NfV encoding in obtaining a desirable trade-off between latency and FER.

In order to validate the conclusion obtained using the bounds, Fig. 5 shows the exact FER for the schemes (i)-(iii), as well as Monte Carlo simulation results for schemes (iv) and (v). While the absolute numerical values of the bounds in Fig. 4 are not uniformly tight with respect to the actual performance evaluated by Fig. 5, the relative performance of the coding schemes in the two figures are well matched. This demonstrates that the derived bounds can serve as a useful tool for code design in NfV systems.

Fig. 6 and Fig. 7 are obtained as Fig. 4 and Fig. 5, respectively, but with the parameters $\mu_1 = 0.02, \mu_2 = 20$, and $a = 0.1$. The key difference with respect to Fig. 4 and Fig. 5 is that, in this regime, repetition coding tends to outperform both uncoded and the NfV code C_c apart from very small latencies. This is because repetition coding has the maximum resilience to the servers unavailability while the latency associated to the larger blocklength n , is dominated here by effects that are independent of n . This is not the case, however, for very small latency levels, where the NfV code C_c provides the smallest FER given its shorter blocklength as compared to repetition coding and its larger d_{\min} with respect to the uncoded scheme.

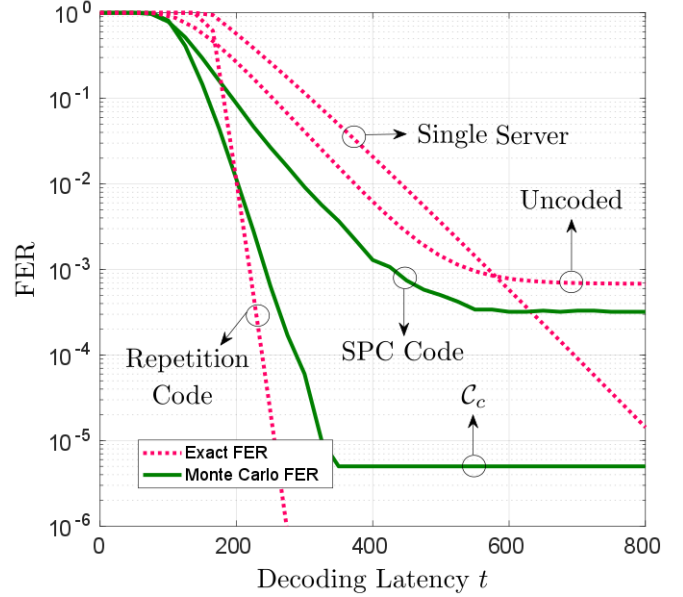


Fig. 7: Exact FER for single-server decoding, repetition coding, uncoded approach and Monte Carlo simulation results for the SPC code and the NfV code C_c defined in (8) ($L = 504, N = 8, 1/\mu_1 = 50, \mu_2 = 20, a = 0.1, \delta = 0.01, r = 0.5$).

V. CONCLUSIONS

In this paper, we analyzed the performance of a novel coded NfV approach for the uplink of a C-RAN system in which decoding takes place at a multi-server or multi-core cloud processor. The approach is based on the linear combination of the received packets prior to their distribution to the servers or cores, and on the exploitation of the algebraic properties of linear channel codes. The method can be thought of as an application of the emerging principle of coded computing to NfV. Analysis and simulation results demonstrate the significant gains that linear coding of received packets, or NfV coding, can yield in terms of trade-off between decoding latency and FER. Among interesting open problems, we mention here the design of optimal NfV codes and the extension of the principle of NfV coding to Gaussian channels.

REFERENCES

- [1] R. Mijumbi, J. Serrat, J.-L. Gorricho, N. Bouten, F. De Turck, and R. Boutaba, "Network function virtualization: State-of-the-art and research challenges," *IEEE Communications Surveys & Tutorials*, vol. 18, no. 1, pp. 236–262, 2016.
- [2] European Telecommunications Standards Institute, "Network functions virtualisation (NFV); reliability; report on models and features for end-to-end reliability," Tech. Rep. GS NFV-REL 003 V1.1.1, Apr. 2016.
- [3] J. Liu, Z. Jiang, N. Kato, O. Akashi, and A. Takahara, "Reliability evaluation for NFV deployment of future mobile broadband networks," *IEEE Wireless Communications*, vol. 23, no. 3, pp. 90–96, 2016.
- [4] J. G. Herrera and J. F. Botero, "Resource allocation in NFV: A comprehensive survey," *IEEE Transactions on Network and Service Management*, vol. 13, no. 3, pp. 518–532, 2016.
- [5] J. Kang, O. Simeone, and J. Kang, "On the trade-off between computational load and reliability for network function virtualization," *IEEE Communications Letters*, 2017.
- [6] J. Dean and S. Ghemawat, "Mapreduce: simplified data processing on large clusters," *Commun. of the ACM*, vol. 51, no. 1, pp. 107–113, 2008.

- [7] K. Lee, M. Lam, R. Pedarsani, D. Papailiopoulos, and K. Ramchandran, "Speeding up distributed machine learning using codes," *Proc. IEEE International Symposium on Information Theory*, pp. 1143–1147, 2016.
- [8] S. Li, M. A. Maddah-Ali, and A. S. Avestimehr, "Fundamental tradeoff between computation and communication in distributed computing," [Online] www.arxiv.org, arXiv:1609.01690 [cs.IT], 2016.
- [9] Y. Yang, P. Grover, and S. Kar, "Computing linear transformations with unreliable components," *IEEE Trans. on Inf. Theory*, 2017.
- [10] T. Rashish, L. Qi, G. D. Alexandros, and K. Nikos, "Gradient coding," [Online] www.arxiv.org arXiv:1612.03301 [cs.IT], 2016.
- [11] S. Dutta, V. Cadambe, and P. Grover, "Short-dot: Computing large linear transforms distributedly using coded short dot products," *Advances In Neural Information Processing Systems*, pp. 2092–2100, 2016.
- [12] A. Severison, A. Graell i Amat, and E. Rosnes, "Block-diagonal coding for distributed computing with straggling servers," [Online] www.arxiv.org, arXiv:1701.06631 [cs.IT], Jan. 2017.
- [13] V. Q. Rodriguez and F. Guillemin, "Towards the deployment of a fully centralized Cloud-RAN architecture," in *IEEE IWCMC*, Spain, 2017.
- [14] A. Al-Shuwaili, O. Simeone, J. Kliewer, and P. Popovski, "Coded network function virtualization: Fault tolerance via in-network coding," *IEEE Wireless Communications Letters*, vol. 5, no. 6, pp. 644–647, 2016.
- [15] S. Janson, "Large deviations for sums of partly dependent random variables," *Random Structures & Algorithms*, vol. 24, no. 3, pp. 234–248, 2004.
- [16] Y. Polyanskiy, H. V. Poor, and S. Verdú, "Channel coding rate in the finite blocklength regime," *IEEE Transactions on Information Theory*, vol. 56, no. 5, pp. 2307–2359, 2010.
- [17] A. Reiszadehmobarakeh, S. Prakash, R. Pedarsani, and S. Avestimehr, "Coded computation over heterogeneous clusters," [Online] www.arxiv.org, arXiv:1701.05973 [cs.IT], 2017.
- [18] A. Sánchez-Arroyo, "Determining the total colouring number is np-hard," *Discrete Mathematics*, vol. 78, no. 3, pp. 315–319, 1989.
- [19] R. L. Brooks, "On colouring the nodes of a network," *Mathematical Proceedings of the Cambridge Philosophical Society*, vol. 37, no. 02, pp. 194–197, 1941.